Available online at www.sciencedirect.com
SCIENCE DIRECT®
Polymer 45 (2004) 3367–3375
polymer
www.elsevier.com/locate/polymer

# Natural rubber latex modification by sodium polyphosphate: a SPM study on the improved latex adhesion to glass sheet

M.M. Rippel, C.A.R. Costa, F. Galembeck*

*Institute of Chemistry, Universidade Estadual de Campinas, P.O. Box 6154, 13083-970 Campinas SP, Brazil*

Received 31 October 2003; received in revised form 2 March 2004; accepted 4 March 2004

**Abstract**

Addition of sodium polyphosphate (NaPP) to natural rubber latex at 0.4 weight ratio improves the adhesion of cast latex dry films to flat glass surfaces. Rubber–polyphosphate dispersions were analyzed by turbidimetric titration, PCS and ultramicroscopy, and the results indicate the formation of two domains within the latex–polyphosphate dispersions: one domain has higher rubber particle content than the other. Thick rubber films were examined by AFM, scanning electric potential and modulated force microscopy. The images show that rubber film morphology is completely altered by NaPP addition. Two types of domains are observed in the dry latex film: one type carries excess positive charges and is harder than the other, negative domains. Both domains are compatible, as shown by the extensive interfaces observed in all images observed. In the latex–glass joints, the positive domains concentrate in the vicinity of the negative glass surface, thus making an electrostatic contribution to glass–latex adhesion.


*Keywords:* Latex–glass adhesion; Colloidal phase separation; Scanning electric potential microscopy

## 1. Introduction

Natural rubber latex (NRL) is a renewable material produced at a very low cost and used in large and growing amounts, in the making of tires, carpet lining, diving gear and adhesives [1]. The latex is an aqueous colloidal dispersion stable at high pH (e.g. due to ammonium hydroxide addition) of rubber (*cis*-1,4 polyisoprene), lutoid and Frey-Wyssling particles, with negative zeta potentials assigned to the adsorbed proteins, phospholipids and fatty acid ammonium salts [2]. Many elements are found in the latex films beyond the C, O, N, S and P associated to the rubber, phospholipids and protein: the presence of Ca, Al, Si, Na, Mg, Mn, Cu and Fe in inorganic particles enclosed in the rubber matrix and/or dispersed throughout the rubber phase has been reported in the literature [3], showing that particles are compatible with rubber through proteins accumulation in the particle–rubber interface.

There are many patents describing the use of natural rubber latex in adhesive formulations. Since the molar weight of the apolar pristine rubber chains is very high, its intrinsic adhesion is low, requiring modification to achieve good adhesion properties in the dry or liquid formulated adhesives. This improvement is reached by graft polymerization with polyolefin [4], copolymerization with vinyl pyrrolidone or vinyl acetate [5], methylmethacrylate and acrylonitrile [6], or mixture with polymeric component containing functional groups suitable for crosslinking [7] or fillers addition [8]. Liquid solvent-based adhesives were widely used but they have been increasingly replaced by water-based dispersions. Previous work from this laboratory showed that the addition of non-crystalline aluminum polyphosphate to a poly(vinyl acetate) (PVAc) latex [9, 10] produces an interpenetrating network with improved wet adhesion to glass. This was interpreted as the result of the formation of aluminum ion bridges across the polyphosphate–rubber interface as well as the glass–rubber and glass–polyphosphate interfaces, which are all formed by negative surfaces.

More recently, we have examined the effect of sodium polyphosphate (NaPP) on natural rubber latex film formation, and we also found an improvement in film adhesion to some substrates, even though monovalent sodium ions cannot make ionic bridges. These results are described in this paper, together with the results of dynamic light

* Corresponding author. Tel./fax: +55-19-3788-3080.
*E-mail address:* fernagal@iqm.unicamp.br (F. Galembeck).

0032-3861/$ - see front matter © 2004 Elsevier Ltd. All rights reserved.
doi:10.1016/j.polymer.2004.03.013

scattering and microscopy experiments, which allowed us to propose a model for the observed adhesion improvement.

## 2. Experimental

### 2.1. Sample preparation

Fresh natural rubber latex was collected from RRIM 600 clone trees at the Instituto Agronômico de Campinas and stored at 5 °C. The latex was centrifuged at 10 krpm for 2 h in a Sorvall RC26 Plus (Du Pont) centrifuge, the upper fraction containing the rubber particles was redispersed in deionized water at 11 wt% solids content, and the pH was adjusted at 10 with aqueous $NH_4OH$. Sodium polyphosphate (Merck, $n_{average} = 20.1$) was weighted and added to the desired amount of natural rubber dispersion ($w_{NaPP}/w_{NRL} = 0.4$), under constant stirring. After homogenization of the mixture for tree hours, films were cast by extending on clean glass sheets [11]. The wet film thickness was 100 μm. The films were air-dried for least 24 h before further analysis.

### 2.2. Turbidimetric titration

This experiment was made to verify the aggregation or coagulation behavior of rubber particles in the presence of sodium polyphosphate. Two milli litres of diluted (0.005 wt%) were added to a quartz cuvette with 4 ml capacity at 25 °C. Aliquots of 100 μl of NaPP solution (25 w/v%) were successively added at 60 s intervals under stirring and resulting turbidity was measured in UV/Vis HP-8452 spectrophotometer at 600 nm.

### 2.3. Dynamic light scattering

The effect of NaPP on the NRL particles was verified by measuring the autocorrelation function of a dispersion containing NRL and NaPP prepared as described in Section 2.1, as a function of time by photon correlation spectroscopy (PCS) using the FOQELS set-up. The FOQELS is a fiber-optic particle sizer designed for use with concentrated suspensions. A 10 mW solid state laser ($\lambda = 670$ nm) is connected to a single-mode optical fiber. The polarized beam impinges on the surface of the sample container and it is collected by another fiber that brings the beam to the detector. The scattering angle is fixed in 155°.

Particles in a liquid are in a random motion, producing fluctuations in the intensity of the scattered light. The scattering intensities are detected in defined time intervals with microsecond's resolution. An autocorrelation function $C(\tau)$ is then obtained:

$$C(\tau) = Ae^{-2\Gamma\tau} + B$$

where $A$ and $B$ are an optical and background constants of the instrument, respectively.

As $\tau$ increases the correlation is lost, and the function approaches to zero. For short times the correlation is high. In this interval, the function decays exponentially for small particle dispersion. However, for a gel or for large particle dispersions $C(\tau)$ does not decay to zero.

### 2.4. Ultramicroscopy

By this technique the sample is observed in an optical microscope dark field while a laser beam illuminates it at 90° to the axis of the objective, and the scattered light is captured through the objective with a video camera [12]. Ultramicroscopy can be used to observe particle motion and clustering, where motion is observed by the displacement of bright spots in the $x-y$ plane and clustering is seen as the concerted motion of neighboring spots. Particle coalescence is observed indirectly by monitoring the disappearance of scattering bright spots. Aggregates of uncoalesced particles are easily observed as clusters of bright spots in the dry film [12].

The light scattering behavior of NRL and NRLPP dispersions was followed by diffusion of 100 μl of each dispersion spread on a 1.5 cm × 1.5 cm glass slide cover kept in a horizontal position. The slide cover was previously washed with ethanol and dried at ambient temperature. The experiment was done within a dark room under (20 ± 1) °C and 46–55% relative humidity. A Bausch&Lomb microscope was used, coupled to a Sony SSC-C350 camera, a Sony PVM-1350 monitor and a JVC HR-S7200U videocassette recorder. Scattered light was used for image formation with a <5 mW and 532 nm diode laser from B&W TEK. The video-recorded images were grabbed using the Pixel View software and processed with Image Pro Plus 4.0.

### 2.5. Adhesion tests

The film–substrate adhesion was qualitatively evaluated by using a sample prepared for the peel test according to ASTM D903 standard, and also by a grid adhesion test according to ASTM D3359. In this test, the sample and control are immersed within a glass container filled with distilled water.

### 2.6. Atomic force microscopy and scanning electric potential microscopy

Films for observation in AFM (non-contact mode) and SEPM were prepared as follows: 5 μl of NRL dispersion were placed over freshly cleaved mica and allowed to dry at room temperature yielding a 7.5 μm thick film. NRLPP films were cast by spreading 100 μl dispersion over cover glasses. Dry films were immersed in water and gently peeled, so that the upper and lower surfaces could be examined. Film thickness was 54 μm. Thicker (134 μm) films were cast for the examination of fracture surfaces: they were dried, peeled, cooled under liquid $N_2$ for 5 min and

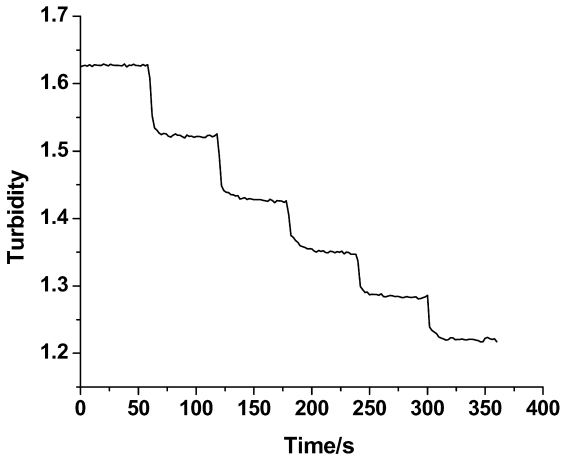


Fig. 1. Turbidimetric titration graphic of the NRL (0.005% in weight). Aliquots of 100 μl NaPP solution (25 w/v%) were added in time intervals of 60 s.

bent. The film fracture surface was mounted parallel to the sample holder surface.

AFM and SEPM images were acquired using a Topometrix Discoverer TMX 2010 as described previously [13–15] and Pt-coated conducting tips with 50 N/m spring constant and 100 kHz resonance frequency.

### 2.7. Modulated force microscopy

This is an imaging method in which the contrast depends on the lateral variations of modulus in the sample. The probe tip is always contacting the sample surface (as in the contact-mode AFM) and a 5 kHz AC wave (well below the tip-cantilever resonance frequency) is applied to the $z$-axis piezoelectric ceramic, with a small amplitude (1–40 Å), so that the sample surface is periodically pushed. The photodetector current produces a DC signal (from which

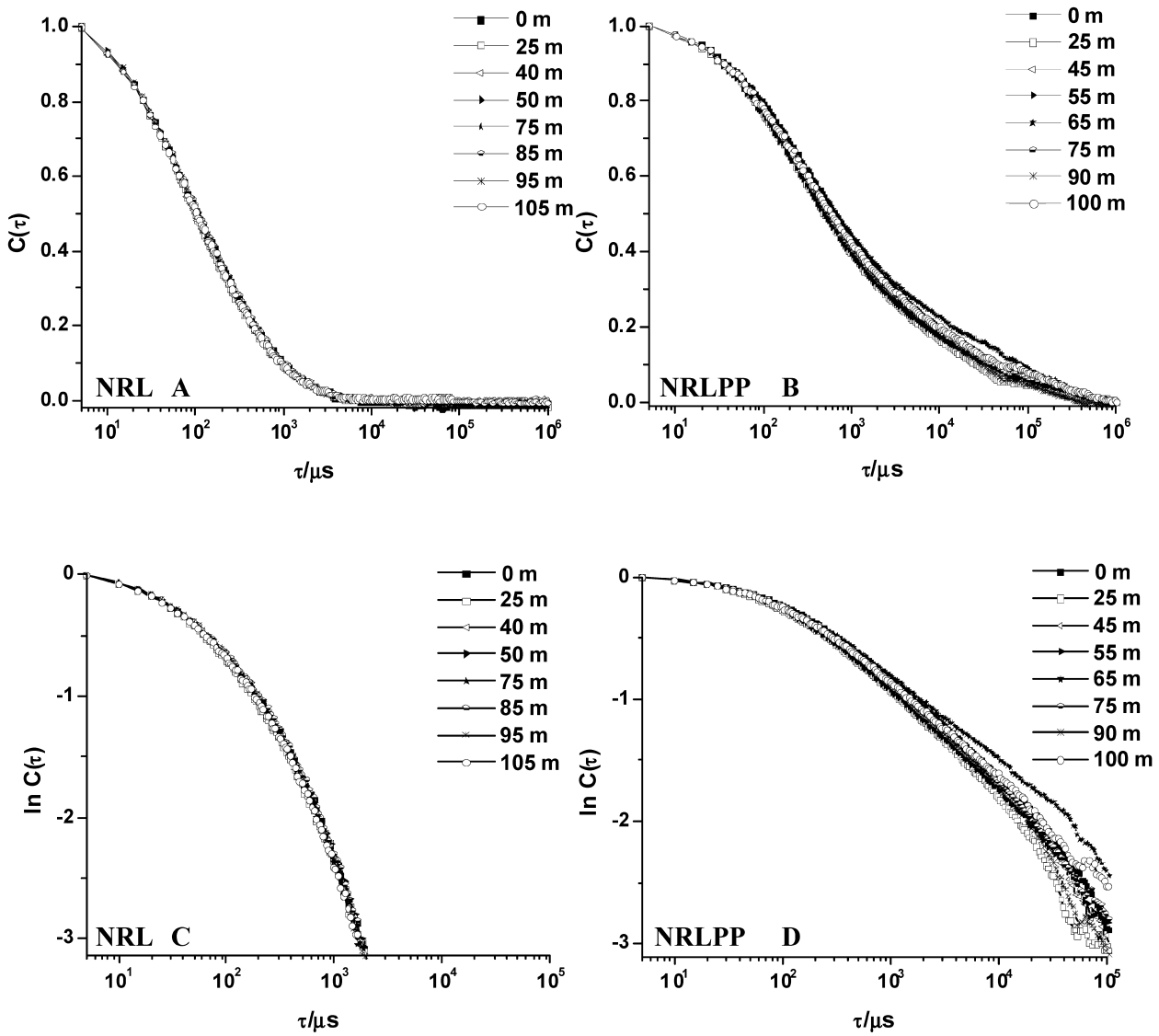


Fig. 2. Normalized autocorrelation functions of the NRL 11% in weight (a) and NRLPP $w_{NaPP}/w_{NRL}$ 0.4 (b) $C$ and $D$ are ln $C(\tau)$ vs. $\tau$ of the normalized autocorrelations functions $A$ and $B$.

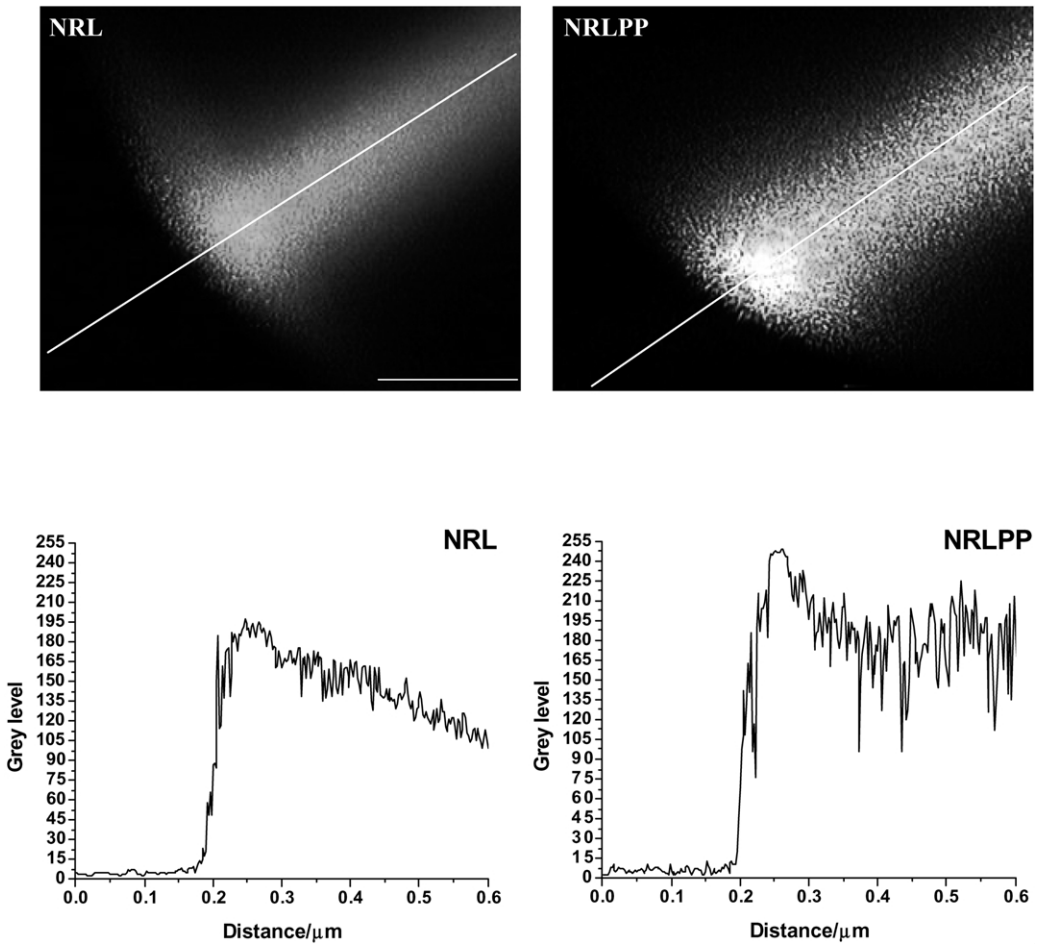


Fig. 3. Ultramicroscopy images of the NRL and NRLPP with laser illumination at 90° and line profiles drawn in the images. Scale bar: 1 mm.

the sample topography is reconstructed) and it contains a 5 kHz component, with an amplitude dependent on the local modulus. Large amplitudes are obtained in soft domains, and vice versa.

### 2.8. Force/distance curves

Information on local sample moduli is also provided by measuring force vs. distance curves, as the probe tip is forced upon the sample surface. In these experiments, the probe is displaced towards the surface and then away from it. Cantilever deflection is measured using the photodetector output, as usual, and knowing its spring constant the force applied by the probe on the surface is determined.

As in any other tension or compression mechanical test, these results depend on many variables, including the rate of probe displacement, cantilever spring constant, temperature, and also on the existence of any contaminating layer built in the surface under the given experimental conditions.

Force distance curves were obtained using Si tips mounted on cantilevers with 3 N/m nominal spring constant.

## 3. Results

The addition of sodium polyphosphate (NaPP) to dilute natural rubber latex does not produce rubber coagulation, even at the highest concentrations used (40% in weight of NaPP), as shown in Fig. 1. The addition of NaPP solution to latex decreases the turbidity due to dilution of dispersion and an increase of the aqueous solvent refractive index. Autocorrelation functions determined for the rubber latex and the rubber–polyphosphate dispersion are given in Fig. 2. There is a marked change in the normalized correlation function $C(\tau)$ : while in NRL, $C(\tau)$ decreases markedly in the $\tau$ (10–100 μs) domain, in the rubber–polyphosphate dispersion $C(\tau)$ varies over the whole $10–10^6$ μs range, evidencing the coexistence of very fast- and very slow-moving light scatterers. Indeed, for some curves (e.g. at 100 m) the value of $C(\tau)$ is still significantly greater than zero, evidencing that a significant fraction of the overall population of scatters is immobile, in this time-scale.

These results show that there are slow changes in the rubber–polyphosphate dispersion, even though there is not observable coagulation. This leads to a hypothesis that is the formation of separate domains in the dispersion, as in a case of colloidal phase separation.

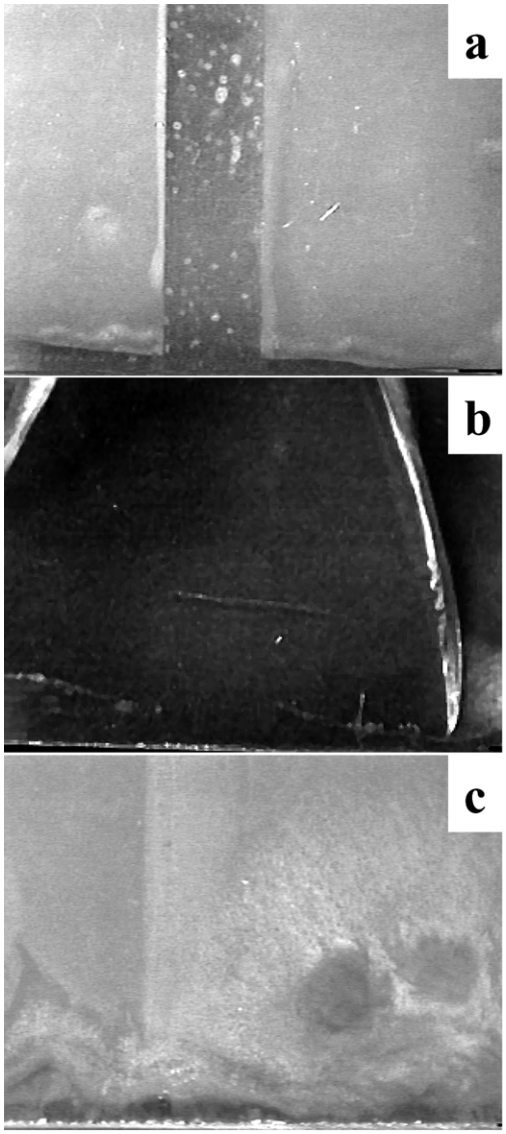


Fig. 4. Tape peel test: (a) film covered with adhesive tape; (b) pristine latex film; (c) polyphosphate–latex film, after the third tape peel.

To verify the presence of different domains in the rubber–polyphosphate dispersion, ultramicroscopy images were obtained and are shown in Fig. 3. The images were obtained in the first 10 s after spreading the samples over the glass sheet. The difference between the light scattering patterns of the rubber and rubber–polyphosphate dispersions is remarkable, as evidenced by the line-scans that are also shown in Fig. 3. The rubber–polyphosphate dispersion shows regions with largely different scattering abilities, in a confirmation of the hypothesis of colloidal phase separation in the rubber–polyphosphate dispersion.

To assess the latex film adhesion ability to glass, rubber and rubber–polyphosphate films were cast on glass sheets. Applying an adhesive tape to the dry NR film and peeling the tape tears the film out of the glass substrate. However, rubber–polyphosphate dry films are undamaged under the same treatment (see Fig. 4), evidencing the increased film-substrate dry adhesion.

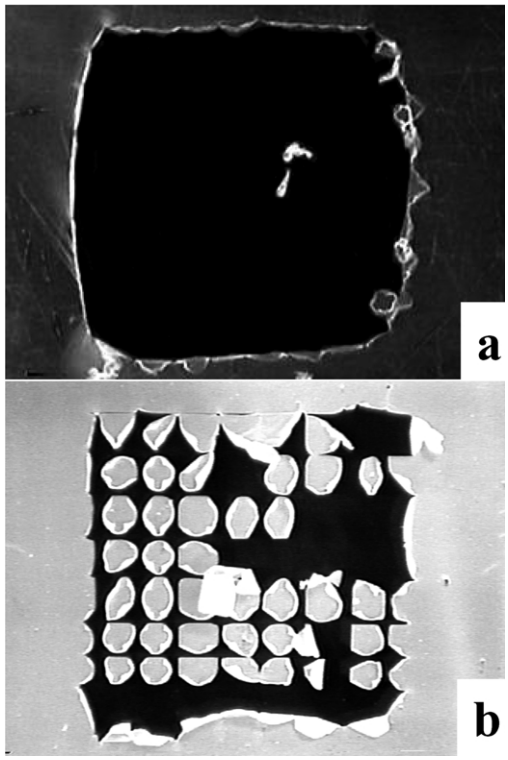


Fig. 5. Wet adhesion test: (a) natural rubber film; (b) natural rubber modified by polyphosphate.

Wet adhesion is also improved, as observed using the grid immersion test (Fig. 5).

The non-contact AFM image of the surface of 7.5 μm-thick latex, shown in Fig. 6, presents two features. First, it has pronounced elevations and depressions, with height differences in excess of 270 nm and thus showing that surface leveling driven by surface tension is far from complete, even though this is a low $T_g$ polymer. The corresponding SEPM image shows that the particle cores are negative, relative to the interparticle domains.

The morphology of the NRLPP films is completely different. Fig. 7 shows the two surfaces of a film formed on glass. The AFM image of the air–film interface still shows elevations, but these are now more diffuse and individual particles are aggregated into larger domains. The SEPM image of the same surface shows large positive patches dispersed in a negative matrix. The positive patches are predominantly coincident with surface depressions, but this association between topography and electric potentials is not as pronounced as in NRL film.

The electric potential gradients in the image plane are remarkably high, reaching 1 V/30 nm, or $3 \times 10^7$ V/m. This is in excess of the known figures for NR dielectric strength, but we should recall that these electric potentials are due to low-mobility ionic constituents in the rubber, without a possibility for electron charge injection in the rubber.

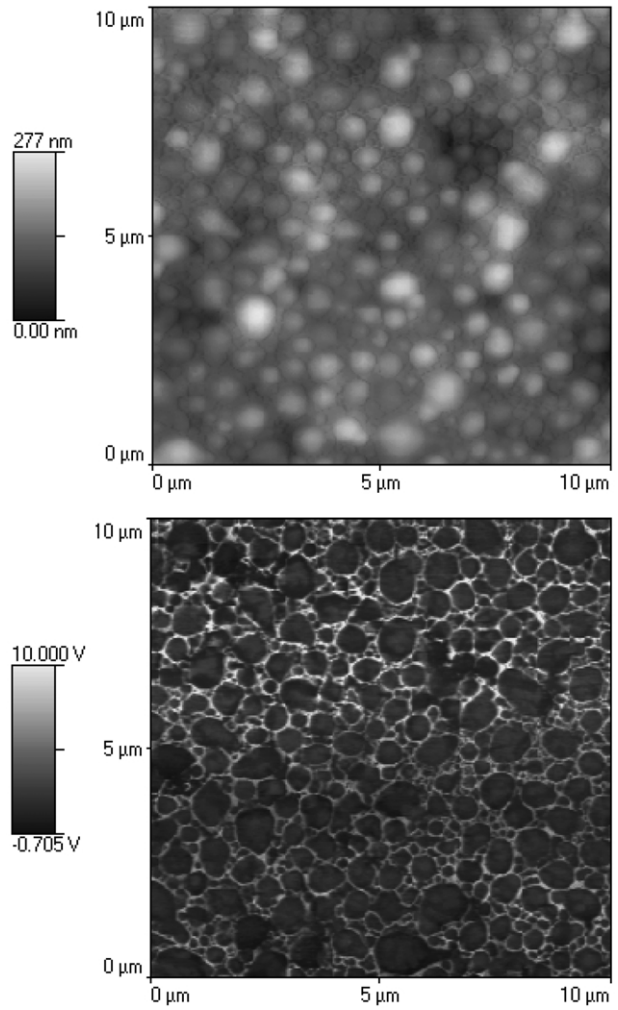


Fig. 6. AFM and SEPM images from NRL film: topography (top) and electric map (bottom).

The film glass interface was obtained after peeling a piece of wet rubber out of the glass, and the respective images are also shown in Fig. 7. Topography is now extremely rough, and the electric domain maps show a large prevalence of positive domains. Moreover, the positive domains are predominantly associated with elevations, while the negative domains are in depressions. This means, the positive domains are always closer to the glass surface than the negative domains.

A complementary view of the glass–NRLPP interface is observed in the images of a fracture surface, shown in Fig. 8. Away from the interface, the bulk rubber film shows the patched domains already seen in Fig. 7, but the glass–rubber interface shows a distinct sandwich structure. The positive glass bulk is covered by a thin negative layer (which is consistent with known zeta potential and adsorption data for glass surfaces), which is then topped by a predominantly positive layer of the positive patchy domains from the rubber. Thus, the accumulation of rubber positive domains close to the glass is observed in the fracture surface, as well as in peeled surface in Fig. 7.

The two major types of domains in the NRLPP films were further characterized by modulated force microscopy (MFM) imaging together with the usual non-contact AFM, as seen in Fig. 9. The patched elevations seen in the non-contact AFM picture appear darker than the continuous, lower matrix, in the MFM picture. Consequently, there is a difference in the moduli of these two types of domains, and the softer (darker) domains are also the positive elevations made out of clustered rubber particles. The elevations borders are harder than the rubber clusters, due to the accumulation of ionic constituents during the drying process [16].

This is confirmed by a different experiment, measuring force vs. distance curves when the microscope tip approaches the rubber surface at different points, as shown in Fig. 10.

In the natural rubber latex film, the modulus calculated from Fig. 10 is low, ca. $0.46 \pm 0.05$ nN/nm, and the measurements made at different film points were always within of this value. However, measurements at different points in the phosphate-modified film were highly variable: in the elevations, the recorded modulus was in the 0.6–0.7 nN/nm range, while in the depressions the moduli calculated from the recorded curves are of the same order of magnitude as the cantilever spring constant, showing that these domains are too hard to be measured with this cantilever. Considering the known deformation modulus of the cantilever, we can state that the modulus of these harder domains exceeds 3 nN/nm.

It should be noted that the hard domains are ca. 0.5 µm beneath the film surface and the overall sample thickness is 54 µm. Consequently, both the hard and soft domains rest on top of a thick composite film that precludes any effect of the mica substrate on these measurements.

## 4. Discussion

The sodium polyphosphate effect on the adhesion of natural rubber latex film is new and unpredicted, and it was only found during a systematic examination of polyphosphate–latex materials. In our previous work on PVA latex–aluminum [10] polyphosphate hybrids, we interpreted the improved adhesion by assuming the formation of aluminum ion bridges between the glass surface and the particles, which are all negatively charged.

This hypothesis cannot prevail in the present case, since the single-charged $Na^+$ ions are unlikely to have the same bridging abilities as the $Al^{3+}$ ions. However, the detailed examination of the dispersions as well as dry films from these samples allow us to put forward a new model, based on (i) colloidal phase separation in the liquid state and (ii) electrostatic interactions between the phase-separated domains in the dry films.

At the high concentrations used, sodium polyphosphate does not induce simple coagulation in the latex, but there is

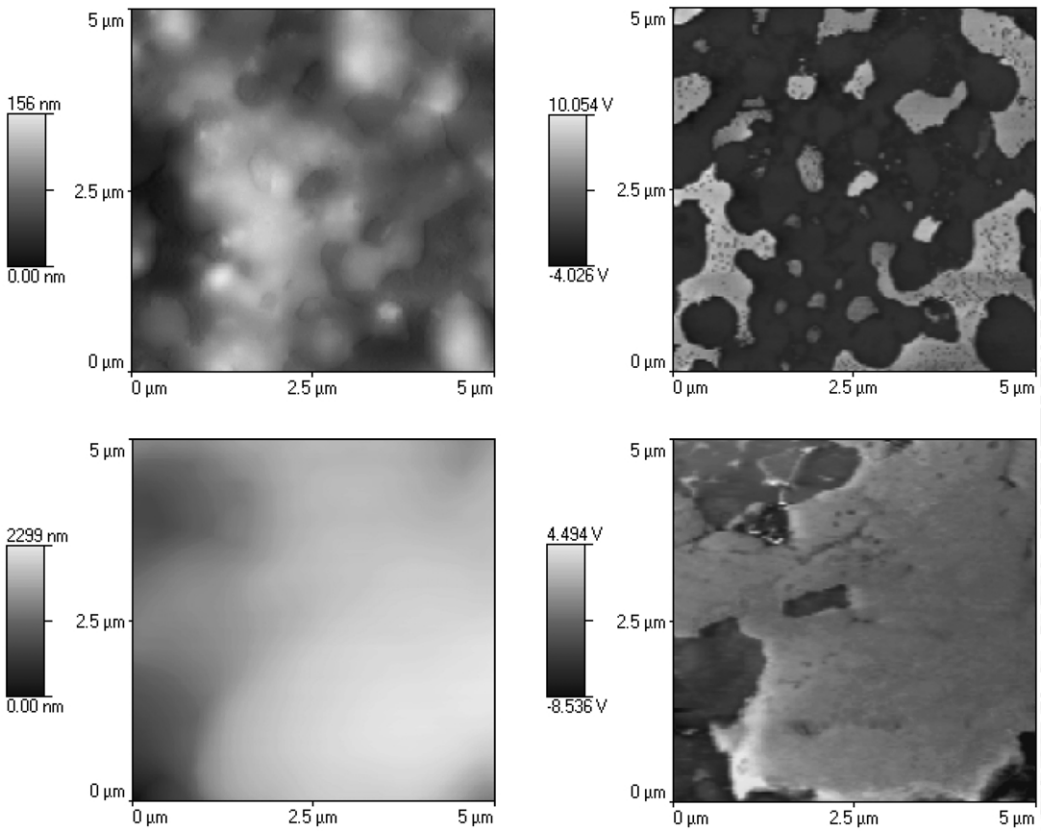


Fig. 7. AFM and SEPM images from NRLPP film: topography (left) and electric map (right). The two upper images are from the surface formed in contact with air, and the bottom images are from the surface formed in contact with glass.

the formation of two (and perhaps more) types of co-existing colloidal domains in the dispersions. Scatterers in these colloidal domains cover a broad range of diffusion coefficients as shown by the autocorrelation functions, showing the coexistence of isolated particles in low-viscosity media and large particle clusters and/or particles in high-viscosity media. The formation of the colloidal domains in the rubber–polyphosphate dispersion is also verified by ultramicroscopy, where the spatial uniformity of distribution of scatterers is much lower than in the pristine latex. AFM, SEPM and MFM techniques all show the coexistence of distinct domains within rubber–polyphosphate dry films. These domains bear largely different electric charge excesses, and since the overall solid is electroneutral, one domain type should be electrically charged opposite to the other domain type. Observation of the domain interfaces in Fig. 7 shows that the two types of domains are quite compatible, since the area of domain interface is extensive as opposed to the quasi-circular shapes observed in incompatible polyphasic materials [17,18]. This is an interesting result, since a biphasic system containing hard and soft domains is created starting with a single polymer and salt.

Glass surfaces in contact with aqueous media are known to acquire a net negative charge, due to sodium ion dissolution, leaving behind excess silicate groups. When the glass is coated with latex, this negative charge is countered by the accumulation of latex domains with excess positive charge at the glass–film interface, as observed in Figs. 7 and 8.

Consequently, we propose that the improved adhesion in this system benefits from an electrostatic contribution made by the opposite charges at the glass and latex film sides of the interface, what in turn depends on the formation and mobility of positively charged latex domains, during film formation and drying.

The colloidal phase separation can be explained considering recent findings on this topic, showing that this is facilitated by electrolytes carrying ions with multiple charges. The observation that flexible counterions with multiple charges destabilize colloidal dispersions of uniform particle concentration provoking colloidal phase separation was described by Linse et al. [19]. The mutual attraction of colloidal particles with similar charge mediated by counterions has been evidenced in different cases by many distinguished authors [20–25]. Ise et al. [24] describe that the higher charge of particles, the stronger the attraction because of the higher availability of counterions. The same argument proved valid in a recent work on liquid–liquid phase separation in an aqueous inorganic salt system [26].

If the observations reported in this paper and the present conclusions are extended to other cases and thus they prove

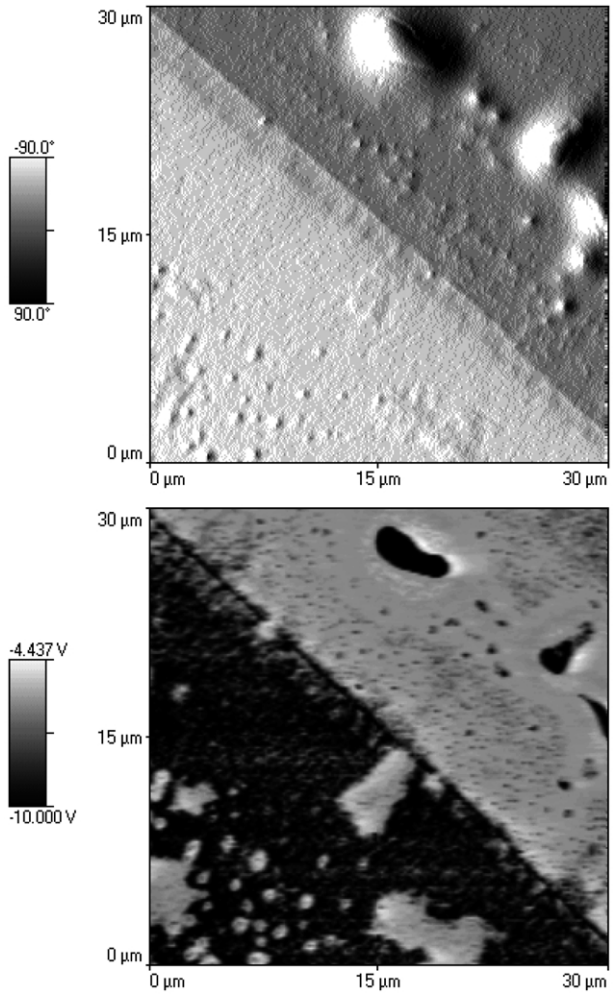


Fig. 8. AFM (top) and SEPM (bottom) images from the NRLPP film/glass joint fracture surface.

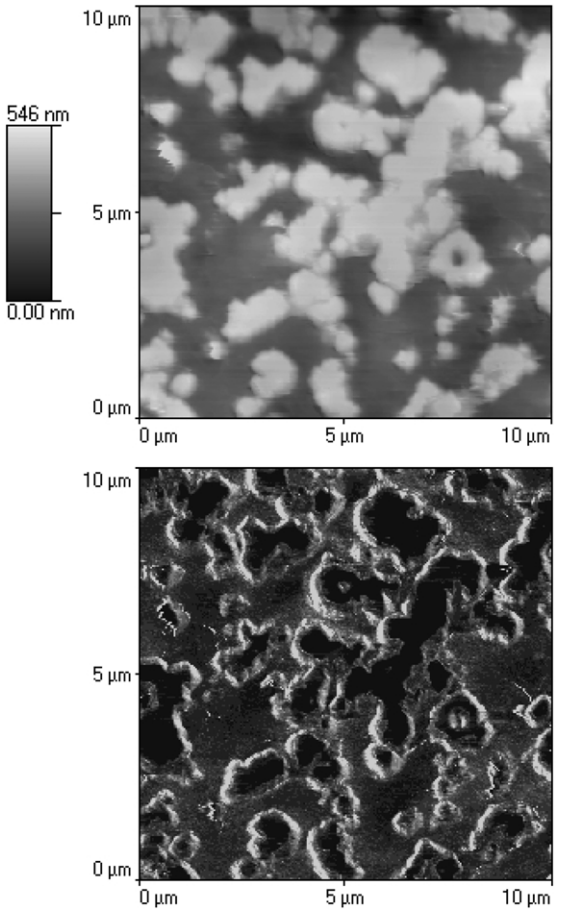


Fig. 9. AFM (top) and modulated force (bottom) images from NRLPP film.

to have some generality, this may allow us to develop some new approaches for solving some existing adhesion problems. However, even if the present results are limited to the present system, they are still interesting as they open new possibilities of practical application for this truly 'green chemistry' latex.

## 5. Conclusions

Sodium polyphosphate addition to natural rubber latex improves the adhesion of the dry latex films to glass, and this is the result of two events:

(i) colloidal phase separation yielding two types of compatible domains with opposite electric charges;
(ii) accumulation of positive rubber film domains close to the negative glass surface, thus making an electrostatic contribution to latex–glass adhesion.

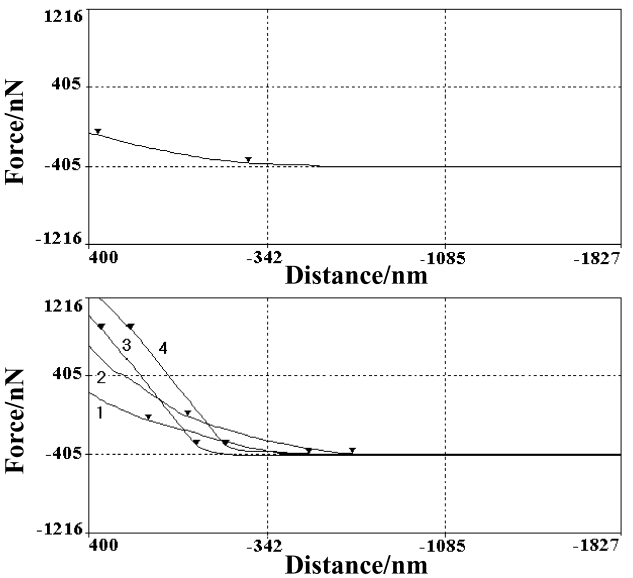


Fig. 10. Nano-indentation force vs. distance curves for NRL film (top) and NRLPP film (bottom). In the latter, curves 1 and 2 were recorded on top of electrically negative domains, and curves 3 and 4 are for positive domains.

## Acknowledgements

M.M.R. is a Fapesp graduate fellow. FG thanks the continuing support of CNPq, Fapesp and Pronex/Finep/MCT. This is a contribution from the Millenium Institute for Complex Materials.

## References

[1] Greve H-H. Rubber Natural. In: Elvers B, Hawkins S, Hussey W, Schulz G, editors. Ullmann's Encyclopedia of Industrial Chemistry, vol. A23. New York: VCH; 1993. p. 225.
[2] Sethuraj MR, Mathew NM. Natural rubber: biology, cultivation and technology. Amsterdam: Elsevier; 1992. p. 80.
[3] Rippel MM, Leite CAP, Galembeck F. Anal Chem 2002;74:2541–6.
[4] Nippon NSC KK. Japanese Patent No. JP2002138266-A; 2002.
[5] Kyodo Printing Co. Japanese Patent No. JP20011354928-A; 2002.
[6] Nippon Zeon KK. Japanese Patent No. JP2001031938-A; 2001.
[7] Griffith WB, Bunn AG, Uhl IE, Ho KS. Rohm & Haas Co. European Patent No. EP1223206-A2; 2003.
[8] Toppan Moore KK. Japanese Patent No. JP2001335769-A; 2003.
[9] Souza EF, Galembeck F. J Mater Sci 1997;32:2207–13.
[10] Souza EF, da Silva MCVM, Galembeck F. J Adhes Sci Technol 1999; 13(3):357–78.
[11] Rippel MM, Galembeck F. Brazil PI No. 2243; 2001.
[12] Keslarek A, Galembeck F. J Appl Polym Sci 2003;87:159–67.
[13] Braga M, Costa CAR, Paula CAP, Galembeck F. J Phys Chem B 2001;105:3005–11.
[14] Galembeck A, Costa CAR, da Silva MCVM, Souza EF, Galembeck F. Polymer 2001;42:4845–51.
[15] Costa CAR, Leite CAP, Galembeck F. J Phys Chem B 2003;107(20): 4747–55.
[16] Lee LT, da Silva MD, Galembeck F. Langmuir 2003;19(17): 6717–22.
[17] Paige MF. Polymer 2003;44(20):6345–52.
[18] Walheim S, Boltau M, Mlynek J, Krausch G, Steiner U. Macromolecules 1997;30:4995–5003.
[19] Linse P, Rescie J. J Phys Chem B 2000;104:7852–7.
[20] Larsen AE, Grier DG. Nature 1997;385:230–3.
[21] Grier DG. Nature 1998;393:621–3.
[22] Bowen WR, Sharif AO. Nature 1998;393:663–5.
[23] Wu JZ, Bratko D, Blanch HW, Prausnitz JM. J Chem Phys 2000;113: 3360–5.
[24] Ise N, Konishi T, Tata BVR. Langmuir 1999;15:4176–84.
[25] Chan DYC, Linse P, Petris SN. Langmuir 2001;17:4202–10.
[26] Azevedo MMM, Bueno MIMS, Davanzo CU, Galembeck F. J Coll Interface Sci 2002;248:185–193.